Appendix: Origin of characteristic X-rays

A.1 Atomic structure

In the Rutherford–Bohr model of the atom, electrons orbit around the nucleus. In the later theory of wave mechanics, orbits are described by *wave functions* representing the probability of finding an electron at a given location. However, the concept of an 'orbital' is still useful and is easier to visualise than an abstract mathematical function. An orbital which represents the spatial probability distribution is defined by quantum numbers as described below. According to Pauli's exclusion principle, only one electron can have a given set of quantum numbers.

The *principal* quantum number is the main determinant of the binding energy and distance from the nucleus of an orbital electron. The inner shells, designated K, L, M, etc., correspond to $n=1,2,3,\ldots$ respectively, the K shell having the greatest binding energy and being closest to the nucleus. The other quantum numbers have a relatively small effect on energy and cause the shells (other than the K shell) to be split into subshells.

The *azimuthal* quantum number l takes values $0,1,2,\ldots,(n-1)$, for a given value of n and represents the angular momentum of the orbital electron. The letters s, p, d, f, etc., used in optical spectroscopy correspond to $l=0,1,2,3$, etc. Thus, for the 3d orbital $n=3$ and $l=2$. A further quantum number s represents the *spin* of the electron and takes values $+1/2$ and $-1/2$. The *total angular momentum* is described by another quantum number j, equal to $l\pm s$ (only positive values allowed). In the case of the L shell ($n=2$), three different combinations of quantum number are possible, giving three subshells:

Subshell	l	j
L_1	0	1/2
L_2	1	1/2
L_3	1	3/2

The number of subshells is equal to $2n-1$: for example the M shell ($n=3$) has five subshells. A complete list of inner shells and their quantum configurations is given in table A.1.

In order to determine the number of electrons occupying each subshell it is necessary to consider yet another quantum number, m_j, which is related to the

Table A.1. *Inner electron shells.*

Shell	n	l	spectroscopic designation	j	Population	Subshell number
K	1	0	1s	1/2	2	—
L	2	0	2s	1/2	2	1
	2	1	2p	1/2	2	2
	2	1	2p	3/2	4	3
M	3	0	3s	1/2	2	1
	3	1	3p	1/2	2	2
	3	1	3p	3/2	4	3
	3	2	3d	3/2	4	4
	3	2	3d	5/2	6	5
N	4	0	4s	1/2	2	1
	4	1	4p	1/2	2	2
	4	1	4p	3/2	4	3
	4	2	4d	3/2	4	4
	4	2	4d	5/2	6	5
	4	3	4f	5/2	6	6
	4	3	4f	7/2	8	7
O	5	0	5s	1/2	2	1
	5	1	5p	1/2	2	2
	5	1	5p	3/2	4	3
	5	2	5d	3/2	4	4
	5	2	5d	5/2	6	5

spatial quantisation of the angular momentum. The different orientations taken up by the angular momentum vector in the presence of an applied magnetic field are represented by the values $j, j-1, \ldots 0, \ldots -j$, of m_j. Normally no such field is present and states with different m_j but the same n, l and j are 'degenerate' – that is they have the same energy. Hence, from Pauli's exclusion principle it follows that the number of electrons occupying a given energy level is $2j+1$: thus the L_1, L_2 and L_3 subshells have populations of 2, 2 and 4 respectively. The populations of other shells are listed in table A.1.

The shell structure is built up by electrons occupying vacant orbitals in order of energy. The K shell, being the most tightly bound, is filled first, and contains two electrons. Next the L shell starts to fill and is complete at $Z=10$. The M shell starts to fill next, but after $Z=18$ the 4s orbital of the N shell has a lower energy than the 3d M-shell orbital and both M and N shells are partially occupied up to $Z=30$, when the M shell is complete. Similar behaviour occurs with other shells at higher atomic numbers, as shown in fig. A.1.

A.2 Characteristic X-ray emission

Electromagnetic radiation is emitted when an orbital electron undergoes a transition between one state (as defined by a set of quantum numbers) and

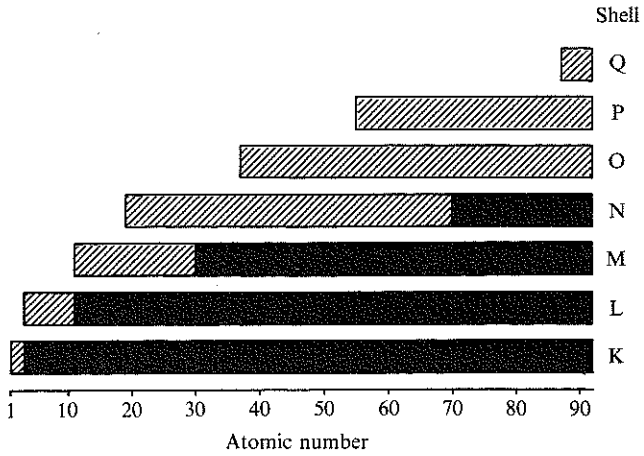

Fig. A.1 Occupancy of atomic shells as function of atomic number: partially filled – shaded, completely filled – black.

another, these states having different energies. The photon energy of the emitted radiation is equal to the difference between these energies and is related to frequency (ν) thus: $E=h\nu$, where h is Planck's constant. The wavelength (λ) is given by: $\lambda=c/\nu$, where c is the velocity of light, hence $E=hc/\lambda$. The usual unit of energy is the electron volt (eV), defined as the energy acquired by an electron when its potential is increased by 1 V, and the practical unit of wavelength is the Ångstrom unit ($1\,\text{Å}=10^{-10}$ m). Using these units, the relationship between energy and wavelength is: $E\lambda=12396$.[1]

X-ray line spectra are produced by electron transitions between inner shells, which are normally fully occupied. A necessary prerequisite for characteristic X-ray emission is the removal of an inner-shell electron, which provides a vacancy or 'hole' into which an electron from a shell further from the nucleus can 'fall'. The vacancy may be produced in various ways, including bombardment with electrons or other charged particles such as protons, or absorption of an X-ray photon. In any case the energy of the incident particle or photon must be greater than the binding energy of the electron concerned. The minimum energy required to produce the vacancy is the 'critical excitation energy' (E_c).

The energy of a characteristic X-ray line is equal to the difference between the energy of the atom in its initial and final states. In the case of the $K\alpha_1$ line, for example, the inner shell of the atom in its initial state is complete except for a vacancy in the K shell. In the final state the vacancy is in the L_3 shell. The energy of the emitted photons is equal to the difference in energy between two levels.

The discussion in §A.1 refers to single electron orbitals, whereas X-ray line emission involves vacancies in otherwise full inner shells. However, Pauli's 'vacancy principle' states that such a vacancy is equivalent to a single electron

[1] This is the value generally used; the updated value of 12398.5 recommended by Jenkins, Manne, Robin and Senemand (1991) is not significantly different from a practical viewpoint.

orbiting an atomic core comprised of the nucleus and complete inner electron shells, enabling the transitions which give rise to X-rays to be treated on the same basis.

Not all transitions are allowed by the rules of quantum theory, according to which the following conditions must be satisfied: $\Delta n\neq 0$, $\Delta l=\pm 1$, $\Delta j=\pm 1$ or 0 (but if $j=0$ initially, then $\Delta j=0$ is forbidden). These are the conditions for 'electric dipole' transitions, which give rise to the principal emission lines. Other types of transition can occur, but with much lower probability. Examples of 'forbidden' lines produced by such transitions are: $K\beta_4$ (K–N_4) and $L\beta_9$ (L_1–M_5).

The atomic states which are relevant to characteristic X-ray production can be represented as horizontal lines on an energy level diagram, in which the zero of the energy scale corresponds to an atom in its rest state with no electrons missing. The energies of the levels associated with the absence of one electron from a shell are positive. The highest level is that of the K shell, since a K electron requires the greatest amount of energy to remove it. Transitions of 'holes' from higher to lower levels giving rise to X-ray emission are described by vertical lines in the energy level diagram. Characteristic X-ray energies may be deduced from the difference in energy between such levels (fig. A.2).

In the usual (Siegbahn) system of line nomenclature, the Greek letters α, β and γ refer to groups of lines of similar wavelength, in order of decreasing

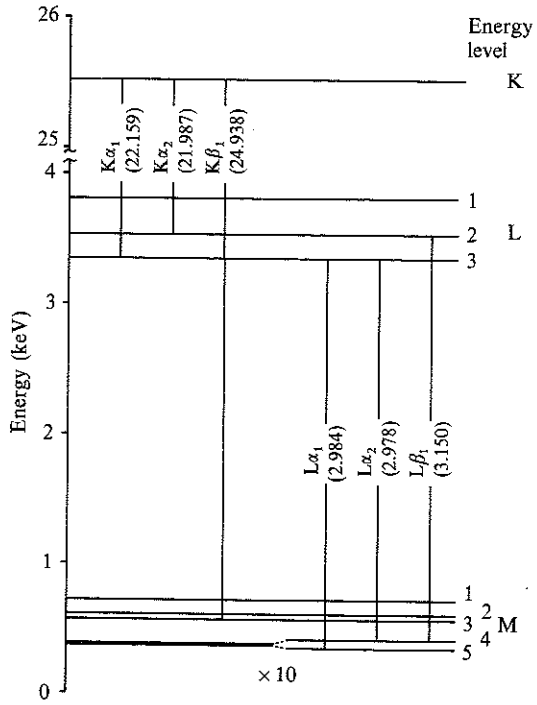

Fig. A.2 Energy level diagram showing K, L and M lines of Ag, and transitions for principal characteristic line (with energies given in keV).

Table A.2. *Initial and final levels for characteristic lines.*

Line	Initial	Final	Line	Initial	Final
$K\alpha_1$	K	L_3	$L\gamma_1$	L_2	N_4
$K\alpha_2$	K	L_2	$L\gamma_2$	L_1	$N_{2,3}$
$K\beta_1$	K	M_3	$L\gamma_3$	L_1	N_3
$K\beta_2$	K	$N_{2,3}$	$L\eta$	L_2	M_1
$K\beta_3$	K	M_2	Ll	L_3	M_1
$L\alpha_1$	L_3	M_5	$M\alpha_1$	M_5	N_7
$L\alpha_2$	L_3	M_4	$M\alpha_2$	M_5	N_6
$L\beta_1$	L_2	M_4	$M\beta_1$	M_4	N_6
$L\beta_2$	L_3	N_5	$M\gamma_1$	M_3	N_5
$L\beta_3$	L_1	M_3	$M\gamma_2$	M_3	N_4
$L\beta_4$	L_1	M_2	$M\delta$	M_2	N_4
$L\beta_5$	L_3	$O_{4,5}$	$M\varepsilon$	M_3	O_5
$L\beta_{15}$	L_3	N_4	$M\xi_1$	M_5	N_3

intensity, while numerical subscripts distinguish the lines within each group, also in decreasing intensity order. There are also some 'odd' lines which fall outside this scheme. Since Greek letters are unsuitable for computers, it is common practice to substitute the equivalent Roman letter (a for α, b for β, etc.). The principal characteristic lines and the corresponding initial and final energy levels are listed in table A.2.

The Siegbahn system was devised before the origin of characteristic X-rays was understood: a more logical approach is to identify the line by the transition which produces it, as recommended by the International Union of Pure and Applied Chemistry (Jenkins *et al.*, 1991). Thus, for example, $K\alpha_1$ becomes K–L_3. However, the older and more familiar system is used here.

A.3 Wavelengths and energies of X-ray lines

Moseley (1913, 1914) noted that the square roots of the frequencies of the Kα lines of different elements lie on a straight line when plotted against atomic number ('Moseley's law'). Using energy in place of frequency, this relationship can be expressed by the equation: $E=a(Z-b)^2$, where a and b are constants. This is a consequence of the dependence of the electron binding energy on the nuclear charge. The constant b is approximately 1 for the Kα lines and represents the reduction in the effective nuclear charge caused by the single remaining K electron. For Lα lines, b has a value of approximately 7.

Moseley's law is not sufficiently accurate to give line energies with high precision: for this purpose it is necessary to use a polynomial expression (e.g. Springer and Nolan, 1976). However, for calculating line energies as required for matrix corrections it is preferable to use tabulated data, since a fitted polynomial may occasionally cause a line to be placed on the wrong side of an absorption edge. Energies and wavelengths can be obtained from tables such as those of White and Johnson (1970). Values for the principal K, L and M lines are listed in tables A.3, A.4 and A.5 respectively.

Table A.3. *Wavelengths (in Å), energies and critical excitation energies (in keV) of K lines (after White and Johnson (1970)).*

		$K\alpha_1$		$K\beta_1$		
Element	Z	λ	E	λ	E	E_c
Be	4	114.0	0.109			0.112
B	5	67.60	0.183			0.192
C	6	44.70	0.277			0.284
N	7	31.60	0.392			0.400
O	8	23.62	0.525			0.532
F	9	18.32	0.677			0.687
Ne	10	14.61	0.848			0.867
Na	11	11.91	1.041	11.62	1.067	1.071
Mg	12	9.890	1.253	9.570	1.295	1.303
Al	13	8.340	1.486	7.982	1.553	1.560
Si	14	7.126	1.739	6.778	1.829	1.840
P	15	6.158	2.013	5.804	2.136	2.143
S	16	5.372	2.307	5.032	2.464	2.470
Cl	17	4.729	2.621	4.403	2.815	2.819
Ar	18	4.193	2.957	3.886	3.190	3.202
K	19	3.742	3.312	3.454	3.589	3.607
Ca	20	3.359	3.690	3.090	4.012	4.037
Sc	21	3.032	4.088	2.780	4.460	4.488
Ti	22	2.750	4.508	2.514	4.931	4.964
V	23	2.505	4.949	2.284	5.426	5.463
Cr	24	2.291	5.411	2.085	5.946	5.988
Mn	25	2.103	5.894	1.910	6.489	6.536
Fe	26	1.937	6.398	1.757	7.057	7.110
Co	27	1.790	6.924	1.621	7.648	7.708
Ni	28	1.659	7.471	1.500	8.263	8.330
Cu	29	1.542	8.040	1.392	8.904	8.979
Zn	30	1.436	8.630	1.295	9.570	9.659
Ga	31	1.341	9.241	1.208	10.26	10.37
Ge	32	1.255	9.874	1.129	10.98	11.10
As	33	1.177	10.53	1.057	11.72	11.86
Se	34	1.106	11.21	0.992	12.49	12.56
Br	35	1.041	11.91	0.933	13.29	13.47

Table A.4. *Wavelengths (in Å), energies and critical excitation energies[a] (in keV) of L lines (after White and Johnson (1970)).*

		$L\alpha_1$		$L\beta_1$		
Element	Z	λ	E	λ	E	E_c
Ga	31	11.29	1.098	11.02	1.125	1.117
Ge	32	10.44	1.188	10.18	1.218	1.217
As	33	9.671	1.282	9.414	1.317	1.323
Se	34	8.990	1.379	8.736	1.419	1.434
Br	35	8.375	1.480	8.125	1.526	1.553
Kr	36	7.817	1.586	7.576	1.636	1.677
Rb	37	7.318	1.694	7.076	1.752	1.806
Sr	38	6.863	1.806	6.624	1.871	1.941
Y	39	6.449	1.922	6.212	1.995	2.079
Zr	40	6.071	2.042	5.836	2.124	2.222
Nb	41	5.724	2.166	5.492	2.257	2.370
Mo	42	5.407	2.293	5.177	2.394	2.523
Ru	44	4.846	2.558	4.621	2.683	2.837
Rh	45	4.597	2.696	4.374	2.834	3.002
Pd	46	4.368	2.838	4.146	2.990	3.172
Ag	47	4.154	2.984	3.935	3.150	3.350
Cd	48	3.956	3.133	3.738	3.316	3.537
In	49	3.772	3.286	3.555	3.487	3.730
Sn	50	3.600	3.443	3.385	3.662	3.928
Sb	51	3.439	3.604	3.226	3.843	4.132
Te	52	3.289	3.769	3.077	4.029	4.341
I	53	3.149	3.937	2.937	4.220	4.558
Xe	54	3.017	4.109	2.806	4.417	4.781
Cs	55	2.892	4.286	2.684	4.619	5.011
Ba	56	2.776	4.465	2.568	4.827	5.246
La	57	2.666	4.650	2.459	5.041	5.483
Ce	58	2.562	4.839	2.356	5.261	5.723
Pr	59	2.463	5.033	2.259	5.488	5.962
Nd	60	2.370	5.229	2.167	5.721	6.208
Sm	62	2.200	5.635	1.998	6.204	6.716
Eu	63	2.121	5.845	1.920	6.455	6.979
Gd	64	2.047	6.056	1.847	6.712	7.242
Tb	65	1.977	6.272	1.777	6.977	7.514
Dy	66	1.909	6.494	1.711	7.246	7.788
Ho	67	1.845	6.719	1.648	7.524	8.066
Er	68	1.784	6.947	1.587	7.809	8.356
Tm	69	1.727	7.179	1.530	8.100	8.648
Yb	70	1.672	7.414	1.476	8.400	8.942
Lu	71	1.620	7.654	1.424	8.708	9.247
Hf	72	1.570	7.898	1.374	9.021	9.556
Ta	73	1.522	8.145	1.327	9.342	9.875
W	74	1.476	8.396	1.282	9.671	10.20
Re	75	1.433	8.651	1.239	10.01	10.53
Os	76	1.391	8.910	1.197	10.35	10.87

Table A.4. (*cont*).

		$L\alpha_1$		$L\beta_1$		
Element	Z	λ	E	λ	E	E_c
Ir	77	1.351	9.174	1.158	10.71	11.21
Pt	78	1.313	9.441	1.120	11.07	11.56
Au	79	1.276	9.712	1.084	11.44	11.92
Hg	80	1.241	9.987	1.049	11.82	12.28
Tl	81	1.207	10.27	1.015	12.21	12.66
Pb	82	1.175	10.55	0.983	12.61	13.04
Bi	83	1.144	10.84	0.952	13.02	13.42

[a] Values given are for the L_3 subshell and apply to the $L\alpha_1$ line only.

Table A.5. *Wavelengths (in Å), energies and critical excitation energies[a] (in keV) of $M\alpha_1$ lines (after White and Johnson (1970)).*

Element	Z	λ	E	E_c
Sm	62	11.47	1.081	
Eu	63	10.96	1.131	
Gd	64	10.46	1.185	
Tb	65	10.00	1.240	
Dy	66	9.590	1.293	
Ho	67	9.200	1.347	
Er	68	8.820	1.405	
Tm	69	8.480	1.462	
Yb	70	8.149	1.521	
Lu	71	7.840	1.581	
Hf	72	7.539	1.644	
Ta	73	7.252	1.709	1.743
W	74	6.983	1.775	1.815
Re	75	6.729	1.842	1.890
Os	76	6.478	1.914	1.968
Ir	77	6.262	1.980	2.049
Pt	78	6.047	2.050	2.134
Au	79	5.840	2.123	2.220
Hg	80	5.648	2.195	2.313
Tl	81	5.460	2.270	2.406
Pb	82	5.286	2.345	2.502
Bi	83	5.118	2.422	2.602
Th	90	4.138	2.996	3.324
U	92	3.910	3.170	3.545

[a] Values not given are very close to the line energy and for practical purposes can be assumed to be the same.

A.4 Relative intensities

Certain predictions about the relative intensities of characteristic X-ray lines can be made. Thus, in the case of the $K\alpha_1$ and $K\alpha_2$ lines the populations of the relevant final energy levels (L_3 and L_2) are in the ratio 2:1, and the observed intensity ratio is in good agreement. For other groups of lines a simplified treatment can be applied, even though different subshells of the same shell are involved, by using the 'Burger–Dorgelo' rule (Compton and Allison, 1935). In the case of the $L\alpha_1$, $L\alpha_2$ and $L\beta_1$ lines, all of which derive from L–M transitions, the L_2 and L_3 levels are first assumed to be merged into a single level, as shown in fig. A.3(*a*). From the populations of the M_4 and M_5 levels it may be deduced that the ratio $L\alpha_1/(L\alpha_2+L\beta_1)$ is equal to 6/4. It is then assumed that the L_2 and L_3 levels are separated, while the M_4 and M_5 levels are merged, as in fig. A.3(*b*), from which it is inferred that $(L\alpha_1+L\alpha_2)/L\beta_1=4/2$. Combining these results, it follows that the intensities of the $L\alpha_1$, $L\alpha_2$ and $L\beta_1$ lines are in the ratio 9:1:5, which is in reasonable agreement with experiment.

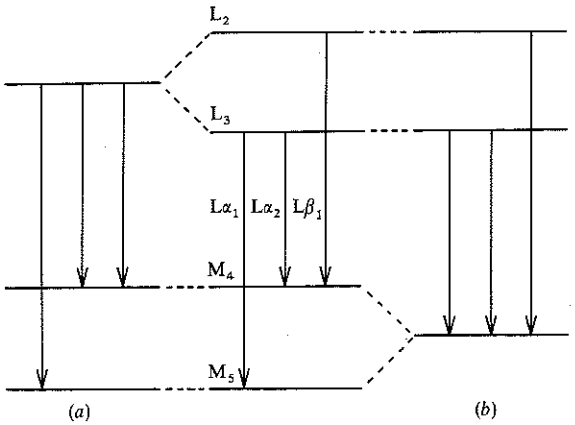

Fig. A.3 Simplified energy level diagrams used in Burger–Dorgelo calculation of relative line intensities (see text).

It should be noted that observed intensities are influenced by incomplete occupancy of the relevant levels. For example, the $K\beta_1/K\alpha_1$ ratio is fairly constant for atomic numbers above about 20, but decreases quite rapidly for lower Z values owing to incomplete filling of the M_3 subshell (the $K\beta_1$ line being produced by the K–M_3 transition). Similar behaviour occurs in the case of L and M lines. Relative line intensities are given by White and Johnson (1970), but in some cases these are only estimated or interpolated values and therefore are not necessarily accurate.

A.5 Satellite lines

Satellite lines do not correspond to any transition identifiable in the energy level diagram and are therefore known as 'non-diagram' lines. The $K\alpha$ line has several satellites on the high energy side, designated $K\alpha'$, $K\alpha_3$, $K\alpha_4$, etc., with

intensities of up to 5% of the main line in the case of Al, for example. These lines are only visible when a w.d. spectrometer is used and even then are usually not fully resolved, appearing as a 'tail' on the short wavelength side of peaks. The $K\beta_1$ line and the principal L and M lines also have satellites.

Satellites are produced by transitions occurring in doubly ionised atoms: for example, a transition from a KL state (with one K and one L electron missing) to an LL state (two L electrons missing). The additional vacancy reduces the screening of the charge on the nucleus, thereby increasing the binding energies of the electrons and shifting the line to a slightly higher energy. Double ionisation may be produced directly by electron bombardment if the incident electrons have sufficient energy, or as a result of the Auger effect (see §A.6).

A.6 Auger effect and fluorescence yield

Inner-shell ionisation does not inevitably lead to characteristic X-ray emission. An alternative possibility is a 'radiationless' transition, whereby the energy released as the electron 'falls' into the initial vacancy is used to eject another electron from the atom. This is known as the 'Auger effect'. Such a transition can be described in terms of the shells containing the initial and final vacancies, e.g. K–L_2L_3. When this occurs, the atom is left in a doubly ionised state. Satellite lines with energies slightly different from the principal lines in the spectrum result from radiative transitions occurring in atoms which are already doubly ionised (§A.5).

The 'fluorescence yield' (ω) is defined as the probability of ionisation of a given shell being followed by characteristic X-ray emission, as opposed to a radiationless Auger transition, and is independent of the means by which the initial vacancy was produced. It can be shown theoretically that the probability of an Auger transition is approximately independent of Z (Wentzel, 1927), whereas the probability of a radiative transition varies as Z^4. The fluorescence yield is thus given approximately by: $\omega=Z^4/(a+Z^4)$. The constant a has a value of about 10^6 for the K shell. The same expression is applicable to other shells, with different values of a. Better accuracy can be obtained with more complicated semi-empirical expressions, such as that proposed by Burhop (1955): $[\omega/(1-\omega)]^{-4}=-A+BZ+CZ^3$. For practical purposes, however, it is probably best to use tabulated values based on experimental data, such as those given in tables A.6 (K shell) and A.7 (L shell).

A.7 Coster–Kronig transitions

In multiple shells a special kind of radiationless transition is possible, involving the transfer of a vacancy from one shell to another. This is known as a 'Coster–Kronig' (C–K) transition. For example, an initial vacancy in the L_1 subshell may move to the L_3 subshell and the energy released be used to eject an M_4 electron. This is described as an L_1–L_3M_4 transition. The C–K process is a special case of the Auger effect and applies to the L and M shells but not the K shell.

For a C–K transition to occur, the ejected outer electron must have a binding energy less than the energy difference between the subshells between which the initial vacancy moves. Thus, in the above case the condition is: $[E(L_1)-E(L_3)]>E(M_4)$, where E represents binding energy. This condition is satisfied for $50>Z>73$. A list of the atomic number ranges for which different L-shell C–K transitions occur is given in table A.8.

Table A.6. *Fluorescence yields for the K shell (after Krause (1979)).*

Element	Z	ω_K	Element	Z	ω_K
B	5	0.0017	Cr	24	0.275
C	6	0.0028	Mn	25	0.308
N	7	0.0052	Fe	26	0.340
O	8	0.0083	Co	27	0.373
F	9	0.013	Ni	28	0.406
Ne	10	0.018	Cu	29	0.440
Na	11	0.023	Zn	30	0.474
Mg	12	0.030	Ga	31	0.507
Al	13	0.039	Ge	32	0.535
Si	14	0.050	As	33	0.562
P	15	0.063	Se	34	0.589
S	16	0.078	Br	35	0.618
Cl	17	0.097	Kr	36	0.643
Ar	18	0.118	Rb	37	0.667
K	19	0.140	Sr	38	0.690
Ca	20	0.163	Y	39	0.710
Sc	21	0.188	Zr	40	0.730
Ti	22	0.214	Nb	41	0.747
V	23	0.243	Mo	42	0.765

Table A.7. *Fluorescence yields for the L subshells (after Krause (1979)).*

Element	Z	ω_{L1}	ω_{L2}	ω_{L3}
Zn	30	0.002	0.011	0.012
Ga	31	0.002	0.012	0.013
Ge	32	0.002	0.013	0.015
As	33	0.003	0.014	0.016
Se	34	0.003	0.016	0.018
Br	35	0.004	0.018	0.020
Kr	36	0.004	0.020	0.022
Rb	37	0.005	0.022	0.024
Sr	38	0.005	0.024	0.026
Y	39	0.006	0.026	0.028
Zr	40	0.007	0.028	0.031
Nb	41	0.009	0.031	0.034
Mo	42	0.010	0.034	0.037
Ru	44	0.012	0.040	0.043
Rh	45	0.013	0.043	0.046
Pd	46	0.014	0.047	0.049
Ag	47	0.016	0.051	0.052
Cd	48	0.018	0.056	0.056
In	49	0.020	0.061	0.060
Sn	50	0.037	0.065	0.064
Sb	51	0.039	0.069	0.069
Te	52	0.041	0.074	0.074

Table A.7. (*cont.*)

Element	Z	ω_{L1}	ω_{L2}	ω_{L3}
I	53	0.044	0.079	0.079
Xe	54	0.046	0.083	0.085
Cs	55	0.049	0.090	0.091
Ba	56	0.052	0.096	0.097
La	57	0.055	0.103	0.104
Ce	58	0.058	0.110	0.111
Pr	59	0.061	0.117	0.118
Nd	60	0.064	0.124	0.125
Sm	62	0.071	0.140	0.139
Eu	63	0.075	0.149	0.147
Gd	64	0.079	0.158	0.155
Tb	65	0.083	0.167	0.164
Dy	66	0.089	0.178	0.174
Ho	67	0.094	0.189	0.182
Er	68	0.100	0.200	0.192
Tm	69	0.106	0.211	0.201
Yb	70	0.112	0.222	0.210
Lu	71	0.120	0.234	0.220
Hf	72	0.128	0.246	0.231
Ta	73	0.137	0.258	0.243
W	74	0.147	0.270	0.255
Re	75	0.144	0.283	0.268
Os	76	0.130	0.295	0.281
Ir	77	0.120	0.308	0.294
Pt	78	0.114	0.321	0.306
Au	79	0.107	0.334	0.320
Hg	80	0.107	0.347	0.333
Tl	81	0.107	0.360	0.347
Pb	82	0.112	0.373	0.360
Bi	83	0.117	0.387	0.373
Th	90	0.161	0.479	0.463
U	92	0.176	0.467	0.489

Table A.8. *Limiting atomic numbers for Coster–Kronig transitions of the type* L_xL_y–M_z.

		z				
x	y	1	2	3	4	5
1	2	<31	<36	<37	<40	<40
1	3	<31	<36	<37	<50	<50
					>73	>77
2	3				<30	<30
						>90

Table A.9. *Coster–Kronig yields for the L shell (after Krause (1979)).*

Element	Z	$f_{1,2}$	$f_{1,2}$	$f_{2,3}$
Zn	30	0.29	0.54	0.03
Ga	31	0.29	0.53	0.03
Ge	32	0.28	0.53	0.05
As	33	0.28	0.53	0.06
Se	34	0.28	0.52	0.08
Br	35	0.28	0.52	0.09
Kr	36	0.27	0.52	0.10
Rb	37	0.27	0.52	0.11
Sr	38	0.26	0.52	0.12
Y	39	0.26	0.52	0.13
Zr	40	0.26	0.52	0.13
Nb	41	0.10	0.61	0.14
Mo	42	0.10	0.61	0.14
Ru	44	0.10	0.61	0.15
Rh	45	0.10	0.60	0.15
Pd	46	0.10	0.60	0.15
Ag	47	0.10	0.59	0.15
Cd	48	0.10	0.59	0.16
In	49	0.10	0.59	0.16
Sn	50	0.17	0.27	0.16
Sb	51	0.17	0.28	0.16
Te	52	0.18	0.28	0.16
I	53	0.18	0.28	0.15
Xe	54	0.19	0.28	0.15
Cs	55	0.19	0.28	0.15
Ba	56	0.19	0.28	0.15
La	57	0.19	0.29	0.15
Ce	58	0.19	0.29	0.15
Pr	59	0.19	0.29	0.15
Nd	60	0.19	0.30	0.15
Sm	62	0.19	0.30	0.15
Eu	63	0.19	0.30	0.15
Gd	64	0.19	0.30	0.15
Tb	65	0.19	0.30	0.15
Dy	66	0.19	0.30	0.14
Ho	67	0.19	0.30	0.14
Er	68	0.19	0.30	0.14
Tm	69	0.19	0.29	0.14
Yb	70	0.19	0.29	0.14
Lu	71	0.19	0.28	0.14
Hf	72	0.18	0.28	0.14
Ta	73	0.18	0.28	0.13
W	74	0.17	0.28	0.13
Re	75	0.16	0.33	0.13
Os	76	0.16	0.39	0.13
Ir	77	0.15	0.45	0.13

Table A.9. (*cont.*)

Element	Z	$f_{1,2}$	$f_{1,2}$	$f_{2,3}$
Pt	78	0.14	0.50	0.12
Au	79	0.14	0.53	0.12
Hg	80	0.13	0.56	0.12
Tl	81	0.13	0.57	0.12
Pb	82	0.12	0.58	0.12
Bi	83	0.11	0.58	0.11
Th	90	0.09	0.57	0.11
U	92	0.08	0.57	0.17

The probability of a vacancy moving from one subshell to another is given by the C–K yield. In the case of the L shell there are three such yields – $f_{1,2}$, $f_{1,3}$ and $f_{2,3}$ – in which the subscripts refer to the initial and final levels. Values for these yields are given in table A.9.

The intensities of L lines involving the L_2 and L_3 levels are enhanced by the transfer of vacancies from L_1 to L_2 and from both L_1 and L_2 to L_3. The enhancement factors are not constant, however, because they depend on the relative numbers of initial vacancies in the subshells, which vary with the excitation conditions. In the case of electron excitation, the ionisation cross-sections depend on the ratio E_0/E_c, and their relative size is a function of E_0. Further, the relative excitation ratios are significantly different for X-ray fluorescence.

The enhancement factors are given by the expressions:

$$1+f_{1,2}n_1/n_2, \text{ for } L_2,$$

and

$$1+(f_{1,3}+f_{1,2}f_{2,3})n_1/n_3+f_{2,3}n_2/n_3, \text{ for } L_3,$$

where n_1, n_2 and n_3 are the production rates of vacancies in the L_1, L_2 and L_3 subshells. For electron excitation these are approximately proportional to the electron populations of these levels, which are 2, 2 and 4 respectively. Enhancement factors can thus be estimated using C–K yields from table A.9: in the case of Ta ($Z=73$), for example, the calculated values are 1.18 for L_2 and 1.22 for L_3. More rigorous estimation requires knowledge of the ionisation cross-sections for the electron energy concerned.

Electron microprobe analysis

SECOND EDITION

S. J. B. Reed
University of Cambridge

CAMBRIDGE
UNIVERSITY PRESS